European Archives of Oto-Rhino-Laryngology (2019) 276:375–382
https://doi.org/10.1007/s00405-018-5249-0

OTOLOGY

Influence of patient-specific anatomy on medical computed tomography and risk evaluation of minimally invasive surgery at the otobasis

Vanessa Schieferbein[1] · Judith Bredemann[2] · R. Schmitt[2] · I. Stenin[1] · T. Klenzner[1] · Jörg Schipper[1] · Julia Kristin[1]

Received: 22 August 2018 / Accepted: 12 December 2018 / Published online: 15 December 2018

Abstract

Purpose With the increasing use of new minimally invasive approaches in temporal bone surgery, the need arises for evaluation of the risk of injury to sensitive anatomical structures. The factors that influence the measurement uncertainty (variation in representation of position and shape of anatomical structures) of imaging are of relevance. We investigate the effect of patients' anatomy on the measurement uncertainty of medical CT.

Methods Six formalin-fixed temporal bones were used, fiducial markers were bone-implanted, and 20 CT scans of each temporal bone were generated. Surgically threatened anatomical structures of importance were defined. Manual segmentation was performed to create 3D surface models, and different Gaussian filters were applied. Analysis points were established along the border of the superior semicircular canal to determine the deviation between the 3D images of the labyrinth. The standard uncertainty was calculated, and one-way analysis of variance was performed (significance level = 5%) to evaluate the effect of certain factors (patient, side, Gaussian filter) on the measurement uncertainty.

Results The influence of patient-specific anatomy on the measurement uncertainty of medical CT ($p = 0.049$) was demonstrated for the first time. The applied Gaussian filter ($p = 0.622$) and the patient's side ($p = 0.341$) showed no significant effect.

Conclusion The applied method and the results of the statistical analysis suggest that the patient's individual anatomical conditions affect the measurement uncertainty of medical CT. Thus, the patient's anatomy must be considered as an important influencing factor during risk evaluation concerning minimally invasive and image-guided surgery.

Keywords Image-guided surgery · Measurement uncertainty · Medical computed tomography · Risk evaluation

Introduction

With increased technology in medicine and more minimally invasive methods, which may reduce postoperative recovery time and tissue damage compared to open access surgery [1, 2], the use of computer-assisted and image-guided surgery is increasing [3].

After presenting minimally invasive access to the cochlea in vitro [3], Labadie et al. recently performed the first clinical realization of an image-guided approach to cochlear implantation using a single drilled tunnel to the middle ear [4] instead of the conventional surgical procedure that requires a wide mastoidectomy. The linear trajectory to the cochlea was planned based on a preoperative CT scan and automatic segmentation to spare important anatomical structures. The defined drilling path was transferred to a second intraoperatively generated CT scan. Intraoperatively fixed fiducials were utilized to facilitate comparison of the patient's anatomy to the CT images. All five drilling channels, used during the in vitro approach, reached the cochlea without injuring the facial nerve. One of five trajectories injured the chorda tympani [3]. The in vivo approach was carried out successfully on five of nine patients. One patient showed a post-operative paralysis of the facial nerve and in three patients, certain difficulties appeared during the insertion of the electrode. Similar approaches of image-guided surgery were performed by different groups [1, 2, 5–8].

✉ Vanessa Schieferbein
vanessa.schieferbein@uni-duesseldorf.de

[1] Department of Otorhinolaryngology, University Hospital Duesseldorf, Duesseldorf, Germany

[2] Laboratory for Machine Tools and Production Engineering WZL, Chair of Production Metrology and Quality Management, RWTH Aachen University, Aachen, Germany

Caversaccio et al. have demonstrated a robotic system that provides an accuracy of 0.15 ± 0.08 mm [2]. Wanna et al. showed an accuracy of 1.02 ± 0.39 mm [7].

Our project, minimally invasive surgery of the otobasis (MUKNO), is currently exploring the possibility of a multiport access to the temporal bone on anatomic specimens that is also based on an image-guided navigation [9]. In this multiport approach, three save trajectories were defined, and boreholes were inserted alongside these paths, leading through the temporal bone and converging at the area of interest. Compared to a single-port approach, the multiport approach allows the utilization of an endoscope and instruments simultaneously and the use for different indications as a result of an increased scope for manipulation and improved visualization [9]. Furthermore, reaching diverse areas of the lateral skull base by the created drilling paths became possible. After manual segmentation of important anatomic structures in the acquired CT images, a special planning tool [10] calculated all the trajectories that will not injure previously selected anatomic structures. From these various trajectories, three save paths can be chosen manually. It has been further investigated whether it is possible to plan nonlinear paths at the lateral skull base [11].

From these new approaches, the question of patients' risk of injury to sensitive anatomical structures arises. This question applies not only to minimally invasive surgery of the lateral skull base, but also to any other kind of computer-assisted and image-guided surgery. Since the lateral skull base contains several critical anatomical structures, such as the facial nerve and internal carotid artery, it provides little space for manipulation. Therefore, extensive preoperative planning and intraoperative navigation using patient-specific CT images are necessary to prevent damage to sensitive structures during minimally invasive methods.

Bredemann et al. [12] purposed a model for assessing the risk of unintentional mechanical injuries during an image-guided surgery of the lateral skull base in the planning phase on a patient-specific basis. The model is based on the assumption that an injury occurs if the planned safety distance between a planned drill trajectory and a risk structure is not large enough to compensate all uncertainties along the surgical process. It has been shown that the major influencing factors for patient's risk are image acquisition and processing, the navigation process and the drilling process and the temperature that is generated during drilling [12]. Uncertainty regarding the robotic system or the drilling process was considered in different approaches [13, 14], and the uncertainty of the navigation process and influencing factors was analyzed by Nau et al. [15].

Another aspect of patient-specific risk that must be taken into consideration is the measurement uncertainty of medical computed tomography and its relevant influencing factors. This uncertainty contribution is especially important, since deviations of the shape and the position of the visualized risk structures from their real shape and position lead to wrong starting conditions for the navigation process. Pollmanns [16] previously reported an approach based on industrial standards to evaluate the uncertainty of medical CT imaging using a specimen composed of material with radiometric characteristics similar to those of human tissues. Although this approach is promising, it remains to be determined whether all the factors that influence the uncertainty of medical CT measurements are covered within the uncertainty approach proposed by Pollmanns. According to Pollmanns u_{img}, the combined measurement uncertainty of medical imaging and image processing is calculated as follows (Eq. 1):

$$u_{\mathrm{img}} = \sqrt{u_{\mathrm{cal}}^2 + u_{\mathrm{p}}^2 + u_{\mathrm{b}}^2 + u_{\mathrm{w}}^2}. \quad (1)$$

The uncertainty u_{img} depends on four different uncertainty contributions: the standard uncertainty of the calibration of the test specimen u_{cal}, the standard uncertainty resulting from the measurement process u_{p}, the standard uncertainty of the correction of the systematic error u_{b} and the standard uncertainty resulting from the variation in size, anatomy and tissue of different patients u_{w}. The contributions u_{cal}, u_{b} and u_{p} were determined with the help of repeat measurements of the test specimen by Pollmanns. Since the concept of measurement uncertainty is widely unknown in the medical domain, the patient's effect on the measurement uncertainty of CT measurements is unknown, but it is reported that there is an influence of the patient size on the quality of head CT [17]. Therefore, u_{w} was estimated within an expert discussion to be roughly 2/3 u_{p} in a first step [16]. To determine the measurement uncertainty of the imaging as precise as possible, it has to be investigated whether there is an influence of the patient on the measurement uncertainty of medical CT measurements. If so, the uncertainty contribution needs to be estimated. In this paper, we show that a significant relationship exists between patient-specific anatomy and the measurement uncertainty of medical computed tomography and quantify the uncertainty contribution.

Materials and methods

Ethical consideration

The study was approved by the local ethics committee (study number: 4713).

Preparation of the anatomic specimen

Three formalin-fixed skull cadavers were used for the research. Five self-tapping titanium screws as fiducials were

fixed to each side of the skull. A CT scan was created using a medical CT scanner (Somatom Definition AS, Software Syngo VA44A, slice thickness 0.6 mm). Twenty scans of each skull were generated and the position of the skull was modified randomly after every scan procedure. This random change of position should simulate different positions of patients during a CT scan to achieve better comparability with daily clinical practice. Anatomical structures that could be damaged during minimally invasive surgery were defined. These structures include the internal carotid artery, jugular vein bulb, facial nerve, chorda tympani, ossicles, cochlea, labyrinth, internal and external auditory canal.

Segmentation

The CT scans were loaded into the segmentation program ITK-Snap freeware [18]. The selected anatomical structures and fiducial markers were manually segmented in each layer of every CT scan to create 3D surface models (Fig. 1). The entire segmentation process was performed by the same person and controlled by a second person to avoid deviations resulting from the involvement of several people. The segmentation was conducted primarily using the axial images. Coronal and sagittal images that were developed by multiplanar reconstruction were used for verification. A Gaussian filter was applied to increase the smoothness of the 3D image. To calculate the filter's influence on measurement uncertainty, the parameter of the smoothing filter was modified. In doing so, three different parameter settings of the filter were used for each segmentation (0; 0.67; 0.8).

Uncertainty estimation

After the segmentation process, the uncertainty of medical CT measurements was estimated for one defined measurement task. Following the work of Pollmanns [16], the determination of the inner diameter of the superior semicircular canal was chosen as the measurement task. Since one of the planned drill trajectories leads through the superior semicircular canal for the scenario of MUKNO surgeries, the determination of this diameter is an important measurement task from a metrological perspective.

Analysis and visualization software, VGSTUDIO MAX 3.0 (Volume Graphics GmbH, Heidelberg, Germany), was used to calculate the deviation between the 3D images of the labyrinth. Therefore, all 20 3D files, including the segmented labyrinth and fiducials, were loaded into the software. The 3D images were overlaid using the fiducials as reference points to align the images correctly. Afterwards, one file was defined as reference data and 12 analysis points were

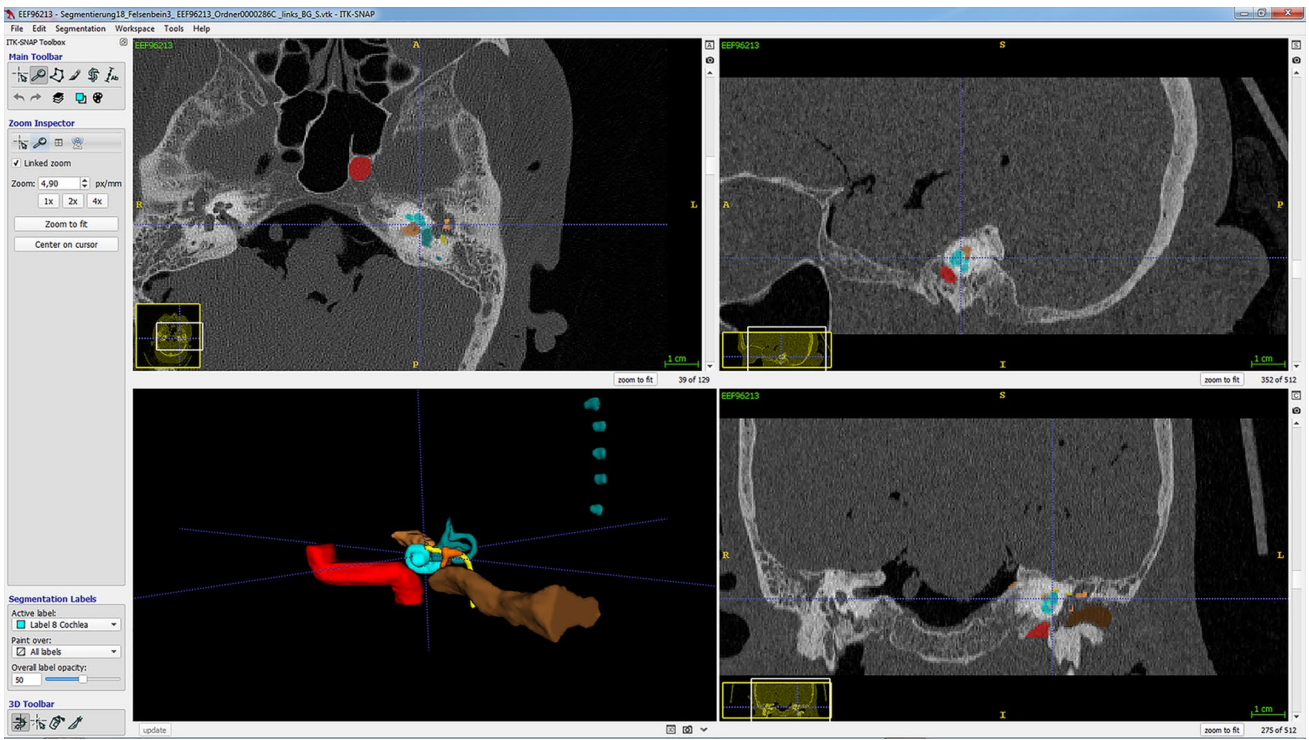

Fig. 1 Screenshot ITK-SNAP: CT image of skull 3, segmentation 18 left. The main window of ITK-SNAP, divided into four areas. Three showing different cross-sections of the input image and the fourth visualizing the 3D view of the segmented structures (red: internal carotid artery, yellow: facial nerve, orange: ossicles, light brown: internal auditory canal, light blue: cochlea, dark blue: labyrinth)

placed along the inner boundary of the superior semicircular canal in the reference data (Fig. 2). The deviation between the reference data and each of the remaining 19 files was calculated based on the analysis points. The resulting measurement values were transferred and the standard uncertainty was calculated for each analysis point. Afterwards, the mean standard deviation was calculated. The entire process was performed on $n = 6$ temporal bones.

Statistics

Statistical analysis was performed using MiniTab statistical software (MiniTab GmbH, Germany). A one-way analysis of variance (ANOVA) was used to evaluate the influence of different factors on measurement uncertainty. The significance level was set at 5%. Investigated influencing factors are as follows: (1) patient, (2) side (right or left), (3) Gaussian filter parameter. The one-way ANOVA is a standard method to determine the influence of parameters on the variance of one or more variables.

Results

The results of the uncertainty analysis for the temporal bone of Patient 1 without Gaussian filter are summarized in Table 1 as an example. Based on the point deviations of the individual repeat measurements, the standard uncertainties of the measurement process are calculated for every analysis point. All standard uncertainties are summarized to the mean measurement uncertainty of the temporal bone. The mean measurement uncertainties of the temporal bones are the basis of the performed ANOVA. Table 2 illustrates the determined measurement uncertainties of each temporal bone.

From the data we obtained, we showed that the specific anatomy of the individual patient affects the measurement uncertainty of medical computed tomography ($p = 0.049$). It

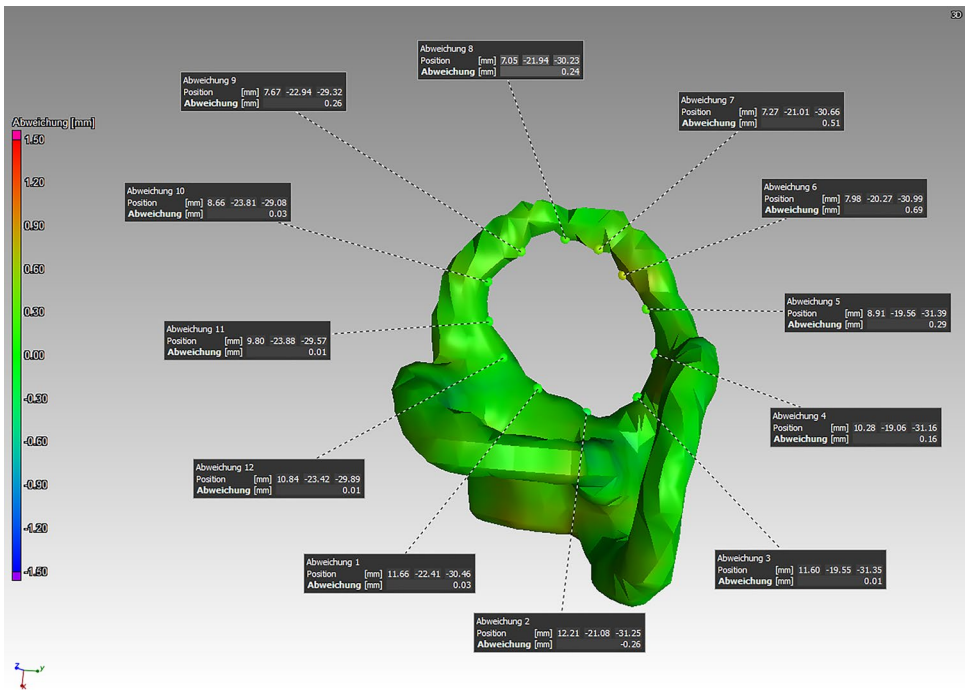

Fig. 2 Screenshot VG Studio Max: 3D image of labyrinth and 12 analysis points along the superior semicircular canal

Table 1 Results of the uncertainty analysis for the temporal bone of Patient 1 (left side, parameter of Gaussian filter: 0)

	Analysis points											
	12	11	10	9	8	7	6	5	4	3	2	1
Standard uncertainty (mm)	0.079	0.127	0.158	0.102	0.104	0.127	0.114	0.136	0.129	0.234	0.246	0.217
Variance (mm^2)	0.006	0.016	0.025	0.010	0.011	0.016	0.013	0.018	0.017	0.055	0.060	0.047
Range (mm)	0.36	0.49	0.59	0.35	0.46	0.50	0.39	0.46	0.58	0.78	1.04	0.83
Mean measurement uncertainty (mm) (analysis points 1–12)	0.157											

Table 2 Determined measurement uncertainties

Patient	Side	Filter	Meas. unc. (mm)
P1	Right	0	0.144
		0.67	0.140
		0.8	0.145
	Left	0	0.157
		0.67	0.162
		0.8	0.169
P2	Right	0	0.226
		0.67	0.290
		0.8	0.328
	Left	0	0.166
		0.67	0.165
		0.8	0.170
P3	Right	0	0.196
		0.67	0.175
		0.8	0.185
	Left	0	0.193
		0.67	0.218
		0.8	0.239

Filter: parameter of Gaussian filter

meas. unc. measurement uncertainty (mm), *P1/P2/P2* patient 1/2/3

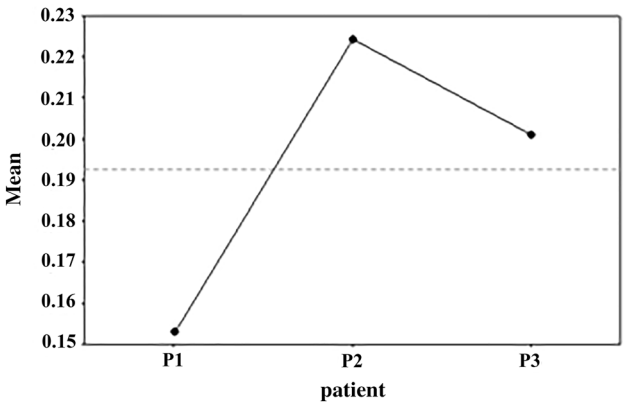

Fig. 3 Main effect plot for measurement uncertainty (patient)

would therefore appear that there is a significant difference between the measurement uncertainties of the individual anatomical specimens. However, in our sample, no difference was detected between the right and left temporal bone of one patient ($p = 0.341$). The applied Gaussian filter (0; 0.67; 0.8), which should increase the smoothness of the 3D images, also showed no significant influence ($p = 0.622$).

For a graphical representation of the statistical calculations, a main effect plot for the different anatomical specimens, the different sides and the different Gaussian filters was created. These main effect plots (Fig. 3) show that a main effect exists for "patient" as the categorical variable.

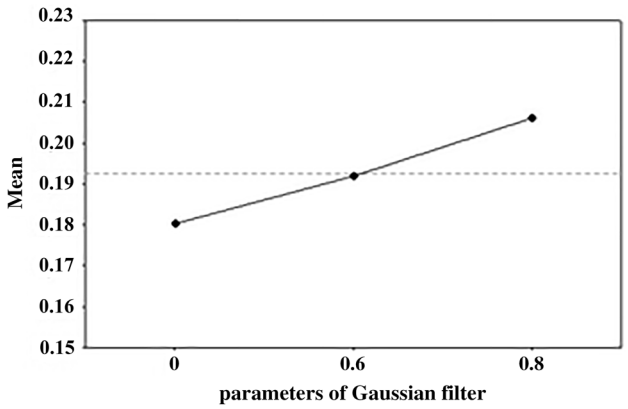

Fig. 4 Main effect plot for measurement uncertainty (filter)

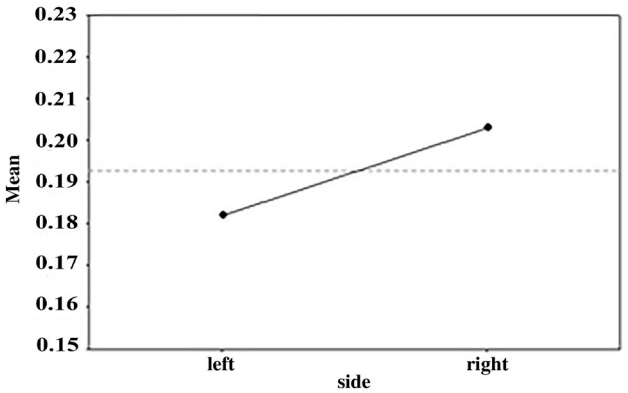

Fig. 5 Main effect plot for measurement uncertainty (side)

The measurement uncertainty is not the same across different patients. The slope of the line between the points indicates the intensity of the main effect. In contrast, the graphs of the main effect plots for "side" and "filter" as variables show a much lower gradient (Figs. 4, 5). This finding agrees with the results of the ANOVA, which determined no effect because of the side or filter.

Since the patient's anatomy does have an influence on the measurement uncertainty, its contribution is estimated based on the results of the uncertainty analysis for the three patients. With the help of the ANOVA, the standard uncertainty resulting from the variation in size, anatomy and tissue of different patients u_w is calculated to be $u_w = 0.05$ mm. The uncertainty of the measurement process u_p is calculated to be 0.24 mm. The uncertainty of the measurement process is the standard deviation of the repeat measurements due to many different influencing factors and components like the X-ray source, the detector, the environment, the user, the software and the data evaluation. Taking into account the uncertainty contributions of the calibration and the uncertainty resulting from systematic errors determined by

Pollmanns ($u_{cal} = 0.005$ mm and $u_b = -0.054$ mm) [16], the uncertainty of the whole imaging process is calculated to be 0.25 mm (see Eq. 1).

Discussion

For the first time, we showed that the patient does influence the measurement uncertainty of medical computed tomography, whereas the Gaussian filter and side of the temporal bone showed no effect in one patient.

The 3D data of anatomical structures, which was necessary for the calculation, was acquired by manual segmentation. Manual segmentation is considered to be the "gold standard" [9], even though it is time consuming and likely not suitable for daily clinical practice. Other possibilities would have been automatic segmentation, such as an atlas-based solution that applies a deforming atlas to perform the segmentation [19]. Stapleford et al. described the possibility of using automatic segmentation [20], and Labadie et al. [4] also used an automatic procedure. However, deviation between the anatomy of the patient and the anatomy of the atlas could produce errors in segmentation [18]. For example, Reda et al. [21] showed that an automatic segmentation program developed for adult patients simply cannot be used to segment pediatric scans. Additionally, automatic segmentation is only truly effective if a large grayscale deviation exists between a structure of interest and the surrounding tissue [22], such a deviation is not always the case. A further point is that automatic segmentation neither allows participation in the process nor the ability to obtain an overview of the patient's anatomy [23]. Another possibility is the use of semiautomatic segmentation programs, e.g., active contour models that are able to trace the contours of anatomical structures automatically when the boundary was selected manually [23]. The usability of these methods is restricted because they are strongly dependent on a large difference in contrast between selected structures and surrounding area, such a difference is not always the case with medical CT images. Additionally, the accuracy of manual segmentation depends on the quality of the image. In our case, because of the resolution of the screen and blurriness of the images, it was sometimes challenging to demarcate the important structures clearly. Furthermore, we used formalin-fixed skulls that differ in certain aspects from living patients.

We used ITK-SNAP software for segmentation because we used this software in the preliminary studies. This software is a free open-source application that is easy to use and does not require mathematical skills [18]. The user interface is well-structured, making it simple to use the program even without having extensive experience. Other segmentation programs may supply additional features, but they frequently include more complicated and unintuitive user interfaces [24]. However, one disadvantage of ITK-Snap is that it is not possible to perform partial volume segmentation [18], resulting in an imprecise representation of very small structures such as the chorda tympani.

The basic thinking behind the implementation and improvement of new minimally invasive and image-guided surgery, such as MUKNO [9] or single-port cochlear implantation [3], is to reduce tissue damage and complication rates for the patient. However, new surgical procedures always raise the question of the resulting risk and are suitable only if the risk is known and does not outweigh the benefits for the patient. Standardized models, which are regularly used in the technical industry, are currently not available for evaluating the risks of surgical interventions at the lateral skull base.

Although there are different studies that define the relevant influencing factors on the surgical risk, the objective of this study is to preoperatively define the general risk for the patient before a "MUKNO-procedure".

To avoid unintended injuries to sensitive structures, the distance between the planned drilling trajectory and the nearest risk structure must be large enough to compensate for uncertainties throughout the surgical process—from the preoperative planning to the drilling of the boreholes. In this context, Bredemann et al. [12] noted three principle errors that influence the risk of unintended mechanical injuries: navigation error, imaging error and drilling process error. By knowing the values of every error, the surgical risk can be calculated for each patient individually when the distance between the planned trajectory and the closest risk structure is known. In our study, we focus on the imaging error that is quantified by the measurement uncertainty of the medical imaging process.

As known from industrial standards, the uncertainty of CT measurements depends on five different uncertainty contributions: the standard uncertainty of the calibration, the standard uncertainty of the drift in the workpiece shape that the calibration referred to, the standard uncertainty resulting from the measurement process, the standard uncertainty of the correction of the systematic error and the standard uncertainty resulting from the variation in materials and production.

Thus, it is known from industrial CT measurements that the workpiece or rather the patient for medical CT measurements can influence the uncertainty of measurement. For example, ten cylinders that were fabricated under similar conditions and fabrication parameters differ in the roughness and form as a result of random influences. If the diameter of the cylinder is measured based on CT images, the differences in form and roughness affect the measurement uncertainty. The same effect is expected when CT measurements are performed for different patients.

We confirmed for the first time that the individual anatomy of a patient influences the measurement uncertainty

of medical computed tomography in a manner similar to the influence of the variation of a workpiece in materials and production. Therefore, the patient's influence has to be included in the calculation of patient risk.

Our study is based on three cadaver heads. From a statistical point of view, this is a relatively small sample. Further studies are necessary to investigate whether the influence can detected more clearly for a larger group of patients when the study covers patients of different sizes and age.

We determined the uncertainty u_w to 0.05 mm which is a smaller contribution than estimated by Pollmanns. The uncertainty budget of the imaging uncertainty needs to be adjusted accordingly. To analyze whether the measurement uncertainty varies with the patient's anatomy, size or tissue properties, detailed analysis of the CT data is necessary which is a part of our further studies. Different measurement tasks and other factors of influence, for instance, the segmentation process will also be analyzed.

Because the imaging error or the uncertainty of medical computed tomography is an important part in calculations of risk during image-guided surgery [25], patient-specific anatomy also affects the risk and should be considered in every kind of risk evaluation.

Against the background of a subsequent use in daily clinical practice, the individual risk of each patient is essential. It should not be forgotten that the development of technical possibilities introduces new, partly unknown risks for the patient. The patient-specific risk will decide whether the use of the minimally invasive method is acceptable for the individual patient, or whether a conventional surgical procedure should be applied.

There are certain inherent risks in minimally invasive and image-guided procedures [26], but by knowing and considering all relevant influencing factors, including the individual patient's anatomy, it becomes possible to prevent complications and increase patient's safety.

Conclusion

To assess the resultant risk during new minimally invasive and image-guided surgical procedures, it is essential to investigate every possible parameter that could affect the intraoperative risk. We showed for the first time that patient-specific anatomical conditions affect the measurement uncertainty of the imaging process and patient-specific risk for damage to essential structures in the temporal bone. Therefore, the influence of patient-specific anatomy should be considered in every kind of risk evaluation regarding the MUKNO procedure or other image-guided surgical approaches. The Gaussian filter that could be applied to smooth the 3D image during segmentation and the patient's side of head showed no effect.

Acknowledgements We would like to thank the German Research Foundation DFG for the support and the funding of the depicted research within the research group MUKNO, the Volume Graphics GmbH for the provision of the software VK STUDIO MAX 3.0 and the image material and the Department for Radiology at the University Hospital Duesseldorf for providing the CT scanner.

Funding This research is funded by the German Research Foundation DFG within the research group MUKNO [SCHI 310/15-2].

Compliance with ethical standards

Ethical consideration The study was approved by the local ethics committee (study number: 4713).

Conflict of interest There is no conflict of interest for Schieferbein, Bredemann, Schmitt, Stenin, Klenzner, Schipper or Kristin.

References

1. Majdani O, Rau TS, Baron S, Eilers H, Baier C, Heimann B, Ortmaier T, Bartling S, Lenarz T, Leinung M (2009) A robot-guided minimally invasive approach for cochlear implant surgery: preliminary results of a temporal bone study. Int J Comput Assist Radiol Surg 4:475–486. https://doi.org/10.1007/s11548-009-0360-8
2. Caversaccio M, Gavaghan K, Wimmer W, Williamson T, Ansò J, Mantokoudis G, Gerber N, Rathgeb C, Feldmann A, Wagner F, Scheidegger O, Kompis M, Weisstanner C, Zoka-Assadi M, Roesler K, Anschuetz L, Huth M, Weber S (2017) Robotic cochlear implantation: surgical procedure and first clinical experience. Acta Otolaryngol 137:447–454. https://doi.org/10.1080/00016489.2017.1278573
3. Labadie RF, Noble JH, Dawant BM, Balachandran R, Majdani O, Fitzpatrick JM (2008) Clinical validation of percutaneous cochlear implant surgery: initial report. Laryngoscope 118:1031–1039. https://doi.org/10.1097/MLG.0b013e31816b309e
4. Labadie RF, Balachandran R, Noble JH, Blachon GS, Mitchell JE, Reda FA, Dawant BM, Fitzpatrick JM (2014) Minimally invasive image-guided cochlear implantation surgery: first report of clinical implementation: minimally invasive image-guided CI Surgery. Laryngoscope 124:1915–1922. https://doi.org/10.1002/lary.24520
5. Ke J, Zhang S-X, Hu L, Li C-S, Zhu Y-F, Sun S-L, Wang L-F, Ma F-R (2016) Minimally invasive cochlear implantation assisted by bi-planar device: an exploratory feasibility study in vitro. Chin Med J 129:2476–2483. https://doi.org/10.4103/0366-6999.191787
6. Labadie RF, Balachandran R, Mitchell J, Noble JH, Majdani O, Haynes D, Bennett M, Dawant BM, Fitzpatrick JM (2010) Clinical validation study of percutaneous cochlear access using patient customized micro-stereotactic frames. Otol Neurotol 31:94–99. https://doi.org/10.1097/MAO.0b013e3181c2f81a
7. Wanna GB, Balachandran R, Majdani O, Mitchell J, Labadie RF (2009) Percutaneous access to the petrous apex in vitro using customized micro-stereotactic frames based on image-guided surgical technology. Acta Otolaryngol 130:1–6
8. Nguyen Y, Miroir M, Vellin J-F, Mazalaigue S, Bensimon J-L, Bernardeschi D, Ferrary E, Sterkers O, Grayeli AB (2011) Minimally invasive computer-assisted approach for cochlear implantation: a human temporal bone study. Surg Innov 18:259–267
9. Stenin I, Hansen S, Becker M, Sakas G, Fellner D, Klenzner T, Schipper J, rg (2014) Minimally invasive multiport surgery of the lateral skull base. Biomed Res Int 2014:379295–379295. https://doi.org/10.1155/2014/379295

10. Stenin I, Hansen S, Becker M, Hirschfeld J, Klenzner T, Schipper J (2012) MUKNO - Multi-Port-Knochenchirurgie am Beispiel der Otobasis - Virtuelle Planung und Machbarkeitsanalyse multiangulärer Bohrkanäle. In: CURAC
11. Fauser J, Sakas G, Mukhopadhyay A (2018) Planning nonlinear access paths for temporal bone surgery. Int J Comput Assist Radiol Surg 13:637–646. https://doi.org/10.1007/s11548-018-1712-z
12. Bredemann J, Voigtmann C, Schmitt R, Stenin I, Kristin J, Klenzner T, Schipper J Determining the patient's risk in minimally invasive surgery to the lateral skull base, vol 155. Universität und Inselspital Bern, Bern
13. Gerber N, Bell B, Gavaghan K, Weisstanner C, Caversaccio M, Weber S (2014) Surgical planning tool for robotically assisted hearing aid implantation. Int J Comput Assist Radiol Surg 9:11–20. https://doi.org/10.1007/s11548-013-0908-5
14. Stenin I, Hansen S, Nau-Hermes M, El-Hakimi W, Becker M, Bredemann J, Kristin J, Klenzner T, Schipper J (2017) Minimally invasive, multi-port approach to the lateral skull base: a first in vitro evaluation. Int J Comput Assist Radiol Surg 12:889–895. https://doi.org/10.1007/s11548-017-1533-5
15. Nau M, Pollmanns S, Schmitt R (2013) Assessing the risk of minimally-invasive surgery: a metrological approach. Int Congr Metrol. https://doi.org/10.1051/metrology/201307002
16. Pollmanns S (2014) Bestimmung von Unsicherheitsbeiträgen bei medizinischen Computertomografiemessungen für die bildbasierte navigierte Chirurgie: Ergebnisse aus der Produktionstechnik. Apprimus Wissenschaftsverlag, Aachen
17. Huda W, Lieberman KA, Chang J, Roskopf ML (2004) Patient size and X-ray technique factors in head computed tomography examinations. I. Radiation doses. Med Phys 31:588–594. https://doi.org/10.1118/1.1646232
18. Yushkevich PA, Piven J, Hazlett HC, Smith RG, Ho S, Gee JC, Gerig G (2006) User-guided 3D active contour segmentation of anatomical structures: significantly improved efficiency and reliability. Neuroimage 31:1116–1128. https://doi.org/10.1016/j.neuroimage.2006.01.015
19. Davatzikos C, Genc A, Xu D, Resnick SM (2001) Voxel-based morphometry using the RAVENS maps: methods and validation using simulated longitudinal atrophy. NeuroImage 14:1361–1369. https://doi.org/10.1006/nimg.2001.0937
20. Stapleford LJ, Lawson JD, Perkins C, Edelman S, Davis L, McDonald MW, Waller A, Schreibmann E, Fox T (2010) Evaluation of automatic atlas-based lymph node segmentation for head-and-neck cancer. Int J Radiat Oncol Biol Phys 77:959–966. https://doi.org/10.1016/j.ijrobp.2009.09.023
21. Reda FA, Noble JH, Rivas A, McRackan TR, Labadie RF, Dawant BM (2011) Automatic segmentation of the facial nerve and chorda tympani in pediatric CT scans. Med Phys 38:5590. https://doi.org/10.1118/1.3634048
22. Strauß G, Hertel I, Dornheim J, Cordes J, Burgert O, Schulz T, Meixensberger J, Winkler D, Preim U, Dietz A, Preim B (2006) Dreidimensionale Darstellung von CT-Datensätzen des Halses für die chirurgische Planung: Eine Machbarkeitsstudie. Laryngorhinootologie 85:746–754. https://doi.org/10.1055/s-2005-921234
23. Schenk A, Prause G, Peitgen H-O (2000) Efficient semiautomatic segmentation of 3D objects in medical images. In: International conference on medical image computing and computer-assisted intervention. Springer, New York, pp 186–195
24. Cates J, Lefohn A, Whitaker R (2004) GIST: an interactive, GPU-based level set segmentation tool for 3D medical images. Med Image Anal 8:217–231. https://doi.org/10.1016/j.media.2004.06.022
25. Widmann G, Stoffner R, Bale R (2009) Errors and error management in image-guided craniomaxillofacial surgery. Oral Surg Oral Med Oral Pathol Oral Radiol Endodontol 107:701–715. https://doi.org/10.1016/j.tripleo.2009.02.011
26. Labadie RF, Davis BM, Fitzpatrick JM (2005) Image-guided surgery: what is the accuracy? Curr Opin Otolaryngol Head Neck Surg 13:27–31